

Title	Strong atomic ordering in Gd-doped GaN
Author(s)	Ishimaru, Manabu; Higashi, Kotaro; Hasegawa, Shigehiko et al.
Citation	Applied Physics Letters. 2012, 101(10), p. 101912
Version Type	VoR
URL	https://hdl.handle.net/11094/89404
rights	This article may be downloaded for personal use only. Any other use requires prior permission of the author and AIP Publishing. This article appeared in Manabu Ishimaru, Kotaro Higashi, Shigehiko Hasegawa, Hajime Asahi, Kazuhisa Sato, and Toyohiko J. Konno, "Strong atomic ordering in Gd-doped GaN", Appl. Phys. Lett. 101, 101912 (2012) and may be found at https://doi.org/10.1063/1.4751245 .
Note	

The University of Osaka Institutional Knowledge Archive : OUKA

<https://ir.library.osaka-u.ac.jp/>

The University of Osaka

Strong atomic ordering in Gd-doped GaN

Cite as: Appl. Phys. Lett. **101**, 101912 (2012); <https://doi.org/10.1063/1.4751245>

Submitted: 13 June 2012 . Accepted: 22 August 2012 . Published Online: 07 September 2012

Manabu Ishimaru, Kotaro Higashi, Shigehiko Hasegawa, Hajime Asahi, Kazuhisa Sato, and Toyohiko J. Konno



[View Online](#)



[Export Citation](#)

ARTICLES YOU MAY BE INTERESTED IN

[Coherent growth of GaGdN layers with high Gd concentration on GaN\(0001\)](#)

Applied Physics Letters **101**, 221902 (2012); <https://doi.org/10.1063/1.4767992>

[Ferromagnetism and its stability in n-type Gd-doped GaN: First-principles calculation](#)

Applied Physics Letters **100**, 232408 (2012); <https://doi.org/10.1063/1.4717243>

[On the magnetic properties of Gd implanted GaN](#)

Journal of Applied Physics **103**, 07D107 (2008); <https://doi.org/10.1063/1.2830644>

Lock-in Amplifiers
up to 600 MHz



Strong atomic ordering in Gd-doped GaN

Manabu Ishimaru,¹ Kotaro Higashi,¹ Shigehiko Hasegawa,¹ Hajime Asahi,¹ Kazuhisa Sato,² and Toyohiko J. Konno²

¹*Institute of Scientific and Industrial Research, Osaka University, Ibaraki, Osaka 567-0047, Japan*

²*Institute for Materials Research, Tohoku University, Sendai, Miyagi 980-8577, Japan*

(Received 13 June 2012; accepted 22 August 2012; published online 7 September 2012)

Gd-doped GaN ($\text{Ga}_{1-x}\text{Gd}_x\text{N}$) thin films were grown on a GaN(001) template by radio frequency plasma-assisted molecular beam epitaxy and characterized by means of x-ray diffraction (XRD) and transmission electron microscopy (TEM). Three samples with a different Gd composition were prepared in this study: $x = 0.02$, 0.05 , and 0.08 . XRD and TEM results revealed that the low Gd concentration GaN possesses the wurtzite structure. On the other hand, it was found that an ordered phase with a quadruple-periodicity along the [001] direction in the wurtzite structure is formed throughout the film with $x = 0.08$. We proposed the atomistic model for the superlattice structure observed here. © 2012 American Institute of Physics. [<http://dx.doi.org/10.1063/1.4751245>]

Diluted-magnetic semiconductors have attracted much attention, because the introduction of the spin degree-of-freedom is anticipated to bring rich functionalities into semiconductor devices.¹ For practical applications of magnetic semiconductors, it is of technological importance to enhance their Curie temperature higher than room temperature. Theoretical studies predicted that transition-metal-doped gallium nitride (GaN) shows ferromagnetism above room temperature,^{2,3} and the room temperature ferromagnetism is experimentally observed in GaCrN (Ref. 4) and GaMnN.⁵ Rare-earth (RE) elements have partially filled *f*-orbitals which give rise to magnetic moments, and therefore they are considered as alternate magnetic dopants for semiconductor materials. In addition, RE-doped GaN shows the sharp luminescence associated with the intra-*f* optical transitions of the RE ions in the visible, which are independent of temperature and almost independent of the host.⁶ From this viewpoint, the GaN-based magnetic semiconductors are promising candidates for semiconductor spintronic devices which can control charges (electrons and holes) and spins as well as photons.

Among a variety of RE elements, gadolinium (Gd) doping of GaN has been extensively studied^{7–12} since Teraguchi *et al.* reported ferromagnetism in $\text{Ga}_{0.94}\text{Gd}_{0.06}\text{N}$ thin films with a Curie temperature of >400 K.¹³ To realize desirable materials properties, it is of technological importance to obtain information on atomic configurations. However, the investigations of structural properties of Gd-doped GaN are relatively limited as compared with those of its magnetic properties. In the present study, we examined atomistic structures of $\text{Ga}_{1-x}\text{Gd}_x\text{N}$ as a function of composition. As a consequence, we found that strong atomic ordering occurs in high Gd concentration GaN.

GaN templates deposited on *c*-axis sapphire (Al_2O_3) wafers were used for the substrate. First, GaN buffer layers were deposited on the templates, then the 250–300 nm-thick $\text{Ga}_{1-x}\text{Gd}_x\text{N}$ thin films were grown at 700 °C by radio frequency (RF) plasma-assisted molecular beam epitaxy. Finally, GaN layers were capped on the top of GaGdN layers as an antioxidant layer. Elemental Ga (purity: 7N) and Gd (3N) and RF plasma-enhanced N_2 were used as sources. During growth, the RF plasma power was 180 W with a nitrogen

flow rate of 1.5 SCCM. The Ga cell temperature was fixed at 861 °C, while the Gd cell temperature changes from 1100 to 1150 °C to control the Gd composition. The samples obtained here were analyzed using x-ray diffraction (XRD) and transmission electron microscopy (TEM). XRD measurements were carried out on a Philips X'pert x-ray diffractometer using Co-K_α radiation (x-ray wave-length of $\lambda = 0.1789$ nm) at 45 kV and 40 mA. Cross-sectional TEM observations were performed using a JEOL JEM-3000F TEM operated at 300 kV. Energy-dispersive x-ray (EDX) spectra were obtained using an ultra-thin-window, energy dispersive x-ray spectrometer manufactured by EDAX. To estimate the Gd composition, Rutherford backscattering spectroscopy analysis is also performed at Toray Research Center. RBS measurements were made using 2.3 MeV He^{2+} beam and a conventional solid-state detector positioned to detect ions backscattered through an angle of 160°. The substrate was oriented 8° off-normal to the incident ion beam in order to minimize channelling effects.

We prepared three samples with a different average Gd composition: “low,” “medium,” and “high” Gd concentration GaN. Figure 1(a) shows XRD profiles, obtained by ω -2 θ scan, as a function of Gd composition. In addition to the Bragg reflections associated with the GaN template and sapphire substrate, the peaks due to epitaxially grown GaGdN thin film are observed in all the specimens. The GaGdN peak is located at the lower angle side of the GaN peak, and their split becomes more pronounced with increasing Gd composition: the lattice parameter of *c*-axis for GaGdN increases with the incorporation of Gd atoms. The features of the profile are almost the same between the low and medium Gd concentration GaN, while it is apparent that additional peaks exist in the profile of the high Gd concentration specimen. The peaks at $2\theta = 35.7^\circ$ and 75.7° can be indexed as GdN 111 and 222 reflections, respectively, suggesting the formation of epitaxially grown GdN precipitates in the GaGdN thin film.¹⁴ On the other hand, the peaks marked with “s” ($2\theta = 9.8^\circ$, 29.7° , 50.5° , and 73.5°) cannot be explained in terms of the possible secondary phases reported so far, such as GdN, Gd_3Ga_2 , and Gd. The details of these “s” peaks are described later.

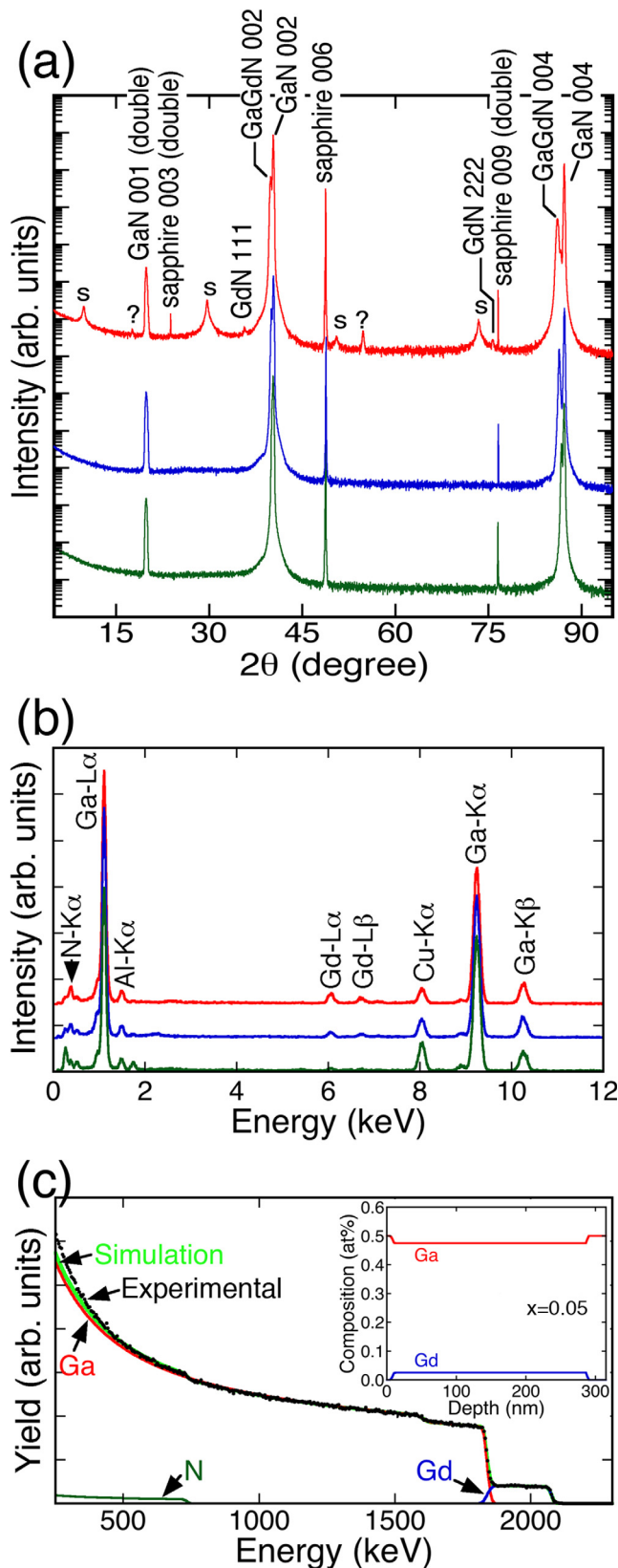


FIG. 1. (a) XRD profiles of $\text{Ga}_{1-x}\text{Gd}_x\text{N}/\text{GaN}/\text{sapphire}$ and (b) EDX spectra of $\text{Ga}_{1-x}\text{Gd}_x\text{N}$ as a function of Gd composition: “low” (bottom), “medium” (middle), and “high” Gd specimens (top). XRD measurements were carried out using $\text{Co-K}\alpha$ radiation (x-ray wave-length of $\lambda = 0.1789 \text{ nm}$). The “double” means the forbidden reflection appearing by double diffraction. The EDX spectra are normalized by the $\text{Ga-K}\alpha$ (9.25 keV) peak. A characteristic x-ray peak of copper originates from the mesh supporting the TEM specimen. (c) RBS spectrum of the high Gd concentration GaN the depth profile of Gd atoms (inset). It is clearly seen that Gd atoms are uniformly distributed within the depth resolution of $\sim 10 \text{ nm}$.

The Gd composition was estimated by TEM equipped with an EDX spectrometer. Stationary probe EDX composition measurements were made using a probe size of $\sim 100 \text{ nm}$. Figure 1(b) shows the EDX profiles of the GaGdN films, which are normalized by the $\text{Ga-K}\alpha$ (9.25 keV) peak. A significant difference is observed in the Gd peak ($\text{Gd-L}\alpha$: 6.06 keV, $\text{Gd-L}\beta$: 6.71 keV). The atomic composition was estimated by integrating the Ga-K and Gd-L peaks. (The N content is certainly underestimated due to strong self-absorption effects for the soft $\text{N-K}\alpha$ x-rays, even in the thinned TEM specimen.) Quantification was carried out with the software “EDAX Genesis” using standard-less analysis and manual background correction. From the quantitative EDX analysis, the composition of $\text{Ga}_{1-x}\text{Gd}_x\text{N}$ was estimated to be $x = 0.02, 0.05$, and 0.08 for the low, medium, and high Gd concentration GaN, respectively. As compared with the Gd composition ($< 10^{20} \text{ cm}^{-3}$) reported by other researchers,¹⁵ a quite large amount of Gd atoms is incorporated in our specimens. To confirm the validity of the EDX results, we also analyzed the high Gd concentration GaN by Rutherford backscattering spectroscopy. Figure 1(c) shows the RBS spectrum and the depth distribution of Ga and Gd atoms (inset). It is clearly seen that the Gd atoms are uniformly distributed in the GaGdN thin film with $x = 0.05$. The RBS results support the remarkable incorporation of Gd atoms in our specimens. Hereafter, we use the Gd composition determined by EDX.

In addition to a rocksalt GdN phase, the formation of an unknown phase was confirmed in $\text{Ga}_{0.92}\text{Gd}_{0.08}\text{N}$ by XRD measurements. To identify the reflections indicated by “s” in Fig. 1(a), cross-sectional TEM observations were performed. Figure 2 shows electron diffraction patterns obtained from

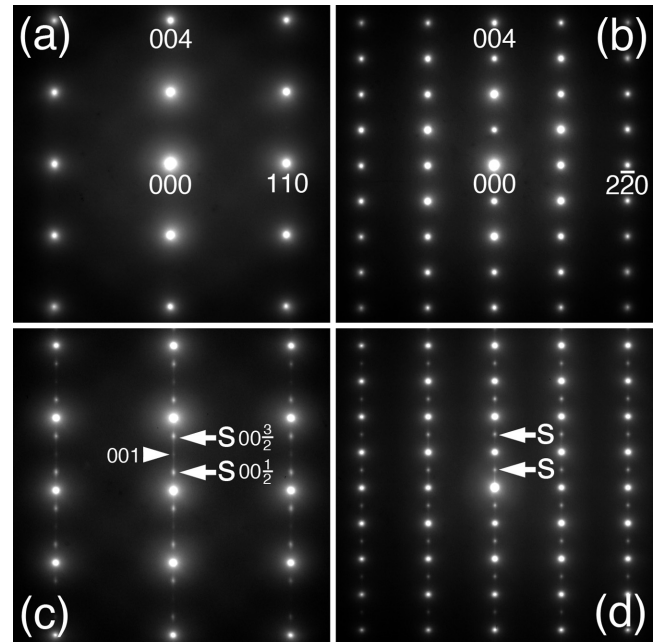


FIG. 2. Electron diffraction patterns of $\text{Ga}_{1-x}\text{Gd}_x\text{N}$ with (a,b) $x = 0.02$ and (c,d) 0.08 . Electron beam is aligned along (a,c) $[1\bar{1}0]$ and (b,d) $[110]$ with respect to the wurtzite GaN structure. The diffraction patterns are indexed as the hexagonal coordinates of the original wurtzite structural unit. The reflections marked with “s” correspond to the unidentified “s” peaks observed in Fig. 1(a). It should be noted that the intensity of the 001 extra reflection indicated by a triangle is much weaker than that of the $00\frac{1}{2}$ and $00\frac{3}{2}$ reflections.

the $\text{Ga}_{1-x}\text{Gd}_x\text{N}$ layer with (a, b) $x = 0.02$ and (c, d) $x = 0.08$. The incident electron beam was focused to a diameter of ~ 200 nm. The diffraction patterns obtained from the low Gd concentration specimen correspond to electron beam orientations (a) $[1\bar{1}0]$ and (b) $[110]$ (hexagonal indices) of the wurtzite structure, and therefore they are indexed in terms of the basic wurtzite structural unit. In addition to the fundamental lattice spots due to the wurtzite structure, extra reflections appear along the $[001]$ direction in the high Gd concentration GaN (Figs. 2(c) and 2(d)). They are located at the one-fourth of two neighboring fundamental Bragg reflections, e.g., 002 and 004, in Fig. 2(c) and their positions are consistent with the “s” peak locations in the XRD profile of Fig. 1(a). This means that quadruple-period atomic ordering along the $[001]$ direction occurs in this specimen. It was confirmed that the same ordered phase is partially formed in $x = 0.05$, though the “s” peaks are not detected in the XRD profile of Fig. 1(a).

It is known that many defects are included in Gd-doped GaN.^{15–17} We have recently found that stacking faults are arranged periodically in Au ion irradiated GaN,¹⁸ and therefore there is a possibility that the similar superlattice-like stacking fault array is formed in Gd-doped GaN. However, it was confirmed that the defects in the present specimens are mainly dislocations and the amount of stacking faults is very low (not shown). This means that the superlattice structure observed here is not due to the periodic arrangement of the defects. To clarify the origin of the superlattice reflections, high-resolution TEM observations were performed. Figure 3 shows the high-resolution TEM images of $\text{Ga}_{0.92}\text{Gd}_{0.08}\text{N}$, viewed along (a) the $[1\bar{1}0]$ and (b) $[110]$ directions. It is apparent that a layer with a bright (or dark) contrast, parallel to the basal plane, exists every ~ 1 nm, and their Fourier power spectra (Figs. 3(c) and 3(d)) are consistent with the

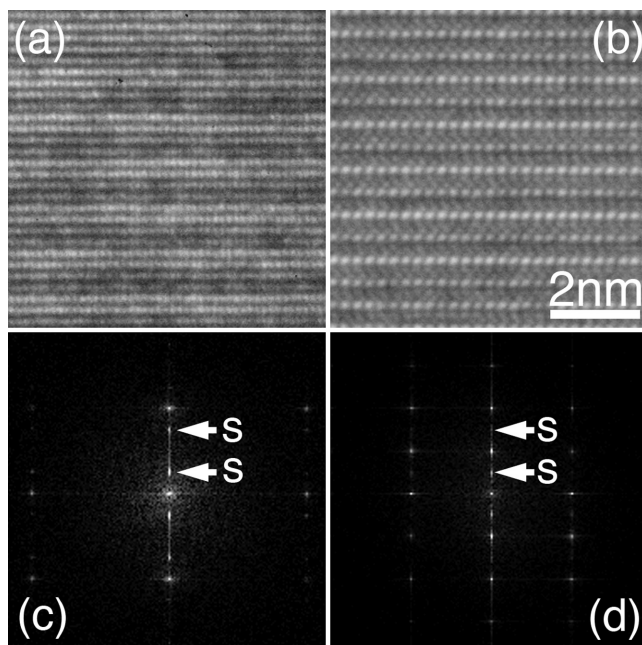


FIG. 3. High-resolution TEM images of $\text{Ga}_{0.92}\text{Gd}_{0.08}\text{N}$, viewed along (a) the $[1\bar{1}0]$ and (b) $[110]$ directions. It is apparent that a modulated structure with a quadruple-periodicity along the $[001]$ direction in the wurtzite structure is formed. (c) and (d) Fast Fourier transforms obtained from the high-resolution TEM images. The diffractograms are in agreement with the electron diffraction patterns of Figs. 2(c) and 2(d).

electron diffraction pattern of Figs. 2(c) and 2(d). It is reported that the third element in GaN sometimes arranges regularly, resulting in the formation of a long-period superlattice structure.^{19–21} We speculate that the superlattice structure in the present study is also induced by the ordered arrangement of the basal planes with a different Gd composition. As described above, the Gd composition is much higher than that reported by other researchers.¹⁵ The remarkable incorporation of Gd atoms into GaN is probably due to the formation of ordered structure.

We propose here an atomistic structural model for the ordered phase. The fundamental lattice spots in the electron diffraction patterns of Figs. 2(c) and 2(d) correspond to those due to the wurtzite structure, and therefore a structural model was constructed based on the wurtzite structure (Fig. 4(a)). The appearance of the superlattice reflections, located at the one-fourth between the 000 and 002 reflections, indicates that the lattice parameter of c -axis is twice as large as that of the original wurtzite structure of GaN. It should be noted that the 001 reflection indicated by a triangle in Fig. 2(c) is very weak as compared with the $00\frac{1}{2}$ and $00\frac{3}{2}$ spots. (The strong 001 reflection in Fig. 2(d) is due to double diffraction.) Figure 4(b) shows a structural model which can reproduce the features of electron diffraction patterns and high-resolution TEM images mentioned above. The lattice parameters are set to be $a = 0.362$ nm and $c = 1.048$ nm, and the atomic positions and compositions are shown as table. The subscript of “ $\text{Ga}_{1-x}\text{Gd}_x$ ” reveals the probability of the site occupancy, and it expresses the color strength in Fig. 4(b). In this model, the compositional modulation is introduced along the c -axis of the wurtzite structure. The average Gd composition is $x = 0.10$, which is nearly the same as that estimated by EDX analysis. The Gd composition at $z = 0.25$ and 0.75 should be nearly equal to the average value of $z = 0$ and 0.5 , in order to satisfy the extinction or very weak intensity of the 001 reflection.

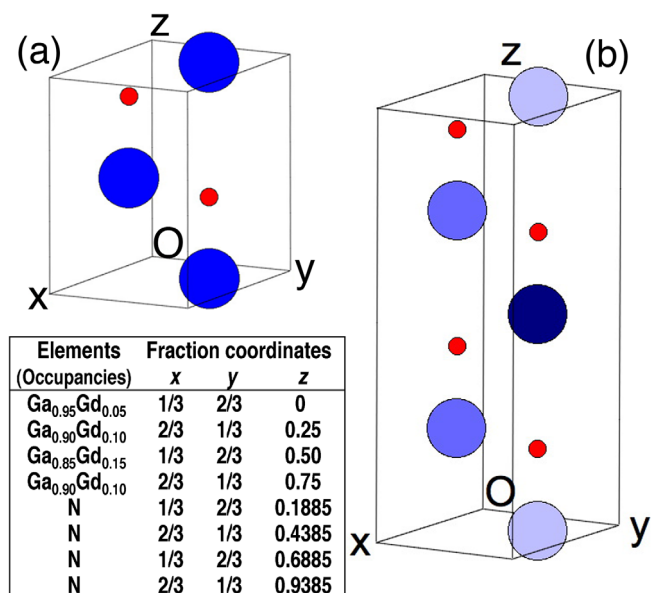


FIG. 4. Atomic configurations of (a) wurtzite and (b) ordered structures. Large and small circles denote $\text{Ga}_{1-x}\text{Gd}_x$ and N, respectively. The table shows the atomic positions and site occupancies in the ordered phase.

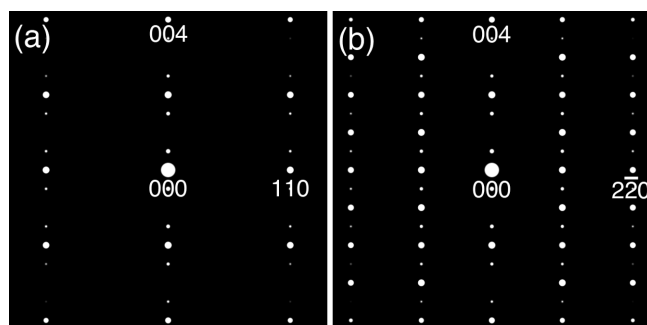


FIG. 5. Simulated electron diffraction patterns for the proposed structure of the unidentified ordered crystalline phase, based on the crystal structure description provided in Fig. 4. Beam orientations are given by (a) $[1\bar{1}0]$ and (b) $[110]$. These diagrams are indexed in terms of the basic wurtzite structural unit. The extinction of 001 reflection in the diagram reproduces the features of the electron diffraction pattern of Fig. 2(c).

Using the model described in Fig. 4(b), we calculated the electron diffraction patterns based on the kinematical approximation, $F_{hkl} = \sum f_n \exp\{2\pi i(hx_n + ky_n + lz_n)\}$, where f_n is the atomic scattering factor for atom n at a fractional coordinate (x_n, y_n, z_n) . Figure 5 shows the resulting diffraction patterns viewed along (a) $[1\bar{1}0]$ and (b) $[110]$. Our proposed structure is likely too simplistic because the deviation from the ideal atomic position of the wurtzite structure, associated with the compositional modulation, is not considered. (This parameter mainly affects the diffraction intensities.) Nevertheless, the agreement between the observed (Figs. 2(c) and 2(d)) and simulated diffraction patterns (Figs. 5(a) and 5(b)) is remarkably good. This suggests that the present structural model is basically correct.

Previous theoretical studies predicted the magnetic properties of diluted-magnetic semiconductors based on the complete random distribution of magnetic elements on the lattice sites. On the other hand, we found experimentally that a strong atomic ordering occurs in Gd-doped GaN. Atomic ordering is often observed in epitaxially grown III-V semiconductor alloys, and it has been reported that the degree of order strongly depends on the growth conditions, such as temperature, composition, and growth rate.^{22–29} Based on this result, there is a possibility that Ga atoms are not randomly substituted with magnetic impurities, but short-range ordered correlation exists even though the degree of order and/or Gd concentration is low. We think the deviation from the complete disordered state affects the prediction of magnetic properties in diluted-magnetic semiconductor materials. In fact, a recent theoretical study showed that the Curie temperature of diluted-magnetic semiconductors is affected by the inhomogeneity of atomistic structures.³⁰

In conclusion, the atomistic structures of $\text{Ga}_{1-x}\text{Gd}_x\text{N}$ /GaN/sapphire were examined by XRD and TEM. In addition to a rocksalt GdN phase, it was found that a strong atomic ordering occurs in high Gd concentration GaN. This ordered phase possesses a compositional modulated structure with a quadruple-periodicity along the $[001]$ direction in the wurtzite structure.

This work was supported by Grant-in-Aid for Scientific Research (C) (Grant No. 22560696) from the Ministry of Education, Sports, Science, and Technology, Japan. TEM observations using a JEOL JEM-3000F were performed at the Comprehensive Analysis Center of ISIR, Osaka University. A portion of this study was performed under the inter-university cooperative research program of the IMR, Tohoku University.

¹H. Ohno, *Science* **281**, 951 (1998).

²T. Dietl, H. Ohno, F. Matsukura, J. Cibert, and D. Ferrand, *Science* **287**, 1019 (2000).

³K. Sato and H. Katayama-Yoshida, *Jpn. J. Appl. Phys. Part 2* **40**, L485 (2001).

⁴M. Hashimoto, Y. K. Zhou, M. Kanamura, and H. Asahi, *Solid State Commun.* **122**, 37 (2002).

⁵G. T. Thaler, M. E. Overberg, B. Gila, R. Frazier, C. R. Abernathy, S. J. Pearton, J. S. Lee, S. Y. Lee, Y. D. Park, Z. G. Khim, J. Kim, and F. Ren, *Appl. Phys. Lett.* **80**, 3964 (2002).

⁶For example, see A. J. Steckl, J. H. Park, and J. M. Zavada, *Mater. Today* **10**, 20 (2007).

⁷H. Asahi, Y. K. Zhou, M. Hashimoto, M. S. Kim, X. J. Li, S. Emura, and S. Hasegawa, *J. Phys.: Condens. Matter* **16**, S5555 (2004).

⁸S. Dhar, L. Pérez, O. Brandt, A. Trampert, K. H. Ploog, J. Keller, and B. Beschoten, *Phys. Rev. B* **72**, 245203 (2005).

⁹L. Pérez, G. S. Lau, S. Dhar, O. Brandt, and K. H. Ploog, *Phys. Rev. B* **74**, 195207 (2006).

¹⁰A. Ney, T. Kammermeier, E. Manuel, V. Ney, S. Dhar, K. H. Ploog, F. Wilhelm, and A. Rogalev, *Appl. Phys. Lett.* **90**, 252515 (2007).

¹¹G. Martínez-Criado, O. Sancho-Juan, N. Garro, J. A. Sans, A. Cantarero, J. Susini, M. Roever, D.-D. Mai, A. Bedoya-Pinto, J. Malindretos, and A. Rizzi, *Appl. Phys. Lett.* **93**, 021916 (2008).

¹²L. Liu, P. Y. Yu, Z. Ma, and S. S. Mao, *Phys. Rev. Lett.* **100**, 127203 (2008).

¹³N. Teraguchi, A. Suzuki, Y. Nanishi, Y. K. Zhou, M. Hashimoto, and H. Asahi, *Solid State Commun.* **122**, 651 (2002).

¹⁴The lattice parameter is slightly different from that of bulk GdN, which is attributed to the lattice constraint by GaGdN matrix.

¹⁵A. Bedoya-Pinto, J. Malindretos, M. Roever, D. D. Mai, and A. Rizzi, *Phys. Rev. B* **80**, 195208 (2009).

¹⁶J. K. Mishra, S. Dhar, and O. Brandt, *Solid State Commun.* **150**, 2370 (2010).

¹⁷J. K. Mishra, B. P. Singh, and S. Dhar, *Appl. Phys. Lett.* **99**, 072119 (2011).

¹⁸M. Ishimaru, I. O. Usov, Y. Zhang, and W. J. Weber, *Philos. Mag. Lett.* **92**, 49 (2012).

¹⁹Z. Liliental-Weber, M. Benamara, J. Washburn, I. Grzegory, and S. Porowski, *Phys. Rev. Lett.* **83**, 2370 (1999).

²⁰M. K. Behbehani, E. L. Piner, S. X. Liu, N. A. El-Masry, and S. M. Bedair, *Appl. Phys. Lett.* **75**, 2202 (1999).

²¹H. K. Cho, J. Y. Lee, K. S. Kim, and G. M. Yang, *Appl. Phys. Lett.* **77**, 247 (2000).

²²A. Gomyo, T. Suzuki, and S. Iijima, *Phys. Rev. Lett.* **60**, 2645 (1988).

²³T. Suzuki, A. Gomyo, S. Iijima, K. Kobayashi, S. Kawata, I. Hino, and T. Yuasa, *Jpn. J. Appl. Phys. Part 1* **27**, 2098 (1988).

²⁴P. Bellon, J. P. Chevalier, E. Augarde, J. P. Andre, and G. P. Martin, *J. Appl. Phys.* **66**, 2388 (1989).

²⁵M. Ishimaru, S. Matsumura, N. Kuwano, and K. Oki, *J. Appl. Phys.* **77**, 2370 (1995).

²⁶M. Ishimaru, S. Matsumura, N. Kuwano, and K. Oki, *Phys. Rev. B* **51**, 9707 (1995).

²⁷M. Ishimaru, S. Matsumura, N. Kuwano, and K. Oki, *Phys. Rev. B* **52**, 5154 (1995).

²⁸M. Ishimaru, S. Matsumura, N. Kuwano, and K. Oki, *Phys. Rev. B* **54**, 10814 (1996).

²⁹M. Ishimaru, Y. Tanaka, S. Hasegawa, H. Asahi, K. Sato, and T. J. Konno, *Appl. Phys. Lett.* **94**, 153103 (2009).

³⁰K. Sato, H. Katayama-Yoshida, and P. H. Dederichs, *Jpn. J. Appl. Phys. Part 2* **44**, L948 (2005).